Chapter

# Interactions of Positrons and Electrons with Hydrogenic Systems, Excitation, Resonances, and Photoabsorption in Two-Electron Systems

*Anand K. Bhatia*

## Abstract

There are a number of approaches to study interactions of positrons and electrons with hydrogenic targets. Among the most commonly used are the method of polarized orbital, the close-coupling approximation, and the *R*-matrix formulation. The last two approaches take into account the short-range and long-range correlations. The method of polarized orbital takes into account only long-range correlations but is not variationally correct. This method has recently been modified to take into account both types of correlations and is variationally correct. It has been applied to calculate phase shifts of scattering from hydrogenic systems like H, $He^+$, and $Li^{2+}$. The phase shifts obtained using this method have lower bounds to the exact phase shifts and agree with those obtained using other approaches. This approach has also been applied to calculate resonance parameters in two-electron systems obtaining results which agree with those obtained using the Feshbach projection-operator formalism. Furthermore this method has been employed to calculate photodetachment and photoionization of two-electron systems, obtaining very accurate cross sections which agree with the experimental results. Photodetachment cross sections are particularly useful in the study of the opacity of the sun. Recently, excitation of the atomic hydrogen by electron impact and also by positron impact has been studied by this method.

**Keywords:** scattering, resonances, photoabsorption, excitation

## 1. Introduction

The discovery of an electron by J.J. Thomson in 1897 led to the development of physics beyond the classical physics. Proton was discovered by Rutherford in 1909. Niels Bohr proposed a model of the structure of hydrogen atoms in 1913. Neutron was discovered by Chadwick in 1932. Other important discoveries were of X-rays and radioactivity in 1896. In 1926, Erwin Schrödinger formulated an equation to determine the wave function of quantum mechanical system. According to Max Born, the wave function can be interpreted as a probability of finding a particle at a specific point in space and time. Many processes could be studied due to such developments in physics. For example, an incoming wave behaves like a particle in

processes like Compton scattering and photoabsorption. Particularly, Geiger and Bothe, using coincident counters, showed that the time between the arrival of the incident wave and the motion of the electron is of the order of $10^{-7}$ second. If the incident wave acted as a wave, the time would have been much longer. Also the experiment of Compton and Simon showed that energy is conserved at every point of the scattering process.

We discuss here scattering of electrons by hydrogenic systems since the wave function of the target is known exactly, and therefore we can test various theories or approximations. When the target consists of more than one electron, a reasonably accurate wave function can only be written using various configurations of the target (called configuration interaction approximation). Among the various approximations for scattering are the exchange approximation [1], the Kohn variational method [2], and the method of polarized orbitals [3] which takes into account the polarization of the target due to the incident electron. The incident electron creates an electric field which results in a change of energy of the target given by $\Delta E = -\frac{1}{2}\alpha E^2$, where $\alpha$ is the polarizabilty of the target and is equal to $4.5\, a_0^3$ in the case of a hydrogen target. The polarization is possible only when the incident electron is outside the target, according to the method of polarized orbitals [3]. However, this method includes only the long-range $-1/r^4$ potential and not the short-range correlations, and the method is not variationally correct. It is possible to use the Feshbach formalism [4] to take into account the short-range correlations via an optical potential. This method gives rigorous lower bonds on the phase shifts, i.e., they are lower than the exact phase shifts. However, it is difficult to include the long-range correlations at the same time. The close-coupling approach takes into account both the long-range and short-range correlations [5] and is variationally correct. However, a large number of target states must be included to obtain converged results and the correct polarizability. A Feshbach resonance below the $n = 2$ threshold of hydrogen atom was first discovered in a close-coupling calculation. A method which has been applied extensively to atomic, molecular, and nuclear physics is the $R$-matrix method introduced by Wigner and Eisenbud in 1947. In this method, configuration space is divided in such a way that all correlations are described within a radius $r = a$, and outside this radius simple continuum functions can be used while matching the inside and outside functions at the boundary $r = a$. This method was introduced in atomic physics by Burke. A method called the hybrid theory [6] has been introduced in which the short-range and long-range correlations are taken into account at the same time and the polarization takes place whether the incident electron is outside or inside the target. This method is variationally correct. The equations for the scattering function are very detailed and are given in [6].

## 2. Scattering function calculations

In the exchange approximation [1], we write the wave function of incident electron and the target as

$$\Psi\left(\vec{r}_1, \vec{r}_2\right) = u\left(\vec{r}_1\right)\phi_0\left(\vec{r}_2\right) \pm (1 \leftrightarrow 2). \tag{1}$$

In the above equation, the plus sign refers to the singlet state, and the minus sign refers to the triplet state, $u\left(\vec{r}_1\right)$ is the scattering function, and

$$\phi_0\left(\vec{r}_2\right) = 2\sqrt{Z^3}e^{-Zr_2}Y_{00}(\hat{r}_2) \tag{2}$$

is the target wave function. The scattering wave function of the incident electron is obtained from

$$\int \left[\phi_0\left(\vec{r}_2\right)|H-E|\Psi\right]d\vec{r}_2 = 0 \tag{3}$$

where $H$ is the Hamiltonian and $E$ is the energy of e-target system. In Rydberg units,

$$H = -\nabla_1^2 - \nabla_2^2 - \frac{2Z}{r} - \frac{2Z}{r_2} - \frac{2}{r_{12}}, \tag{4}$$

$$E = k^2 - Z^2, \tag{5}$$

where $k^2$ is the kinetic energy of the incident electron and $Z$ is the nuclear charge of the target, assumed fixed. The scattering equation is

$$\begin{aligned}&\left[\frac{d^2}{dr_1^2} - \frac{l(l+1)}{r_1^2} + 2e^{-2Zr_1}\left(1+\frac{1}{r_1}\right) + k^2\right]u_l(r_1)\\ &\pm 4Z^3e^{-Zr_1}\left[\left(Z^2+k^2\right)\delta_{l0}r_1\int_0^\infty e^{-Zr_2}r_2u_l(r_2)dr_2 - \frac{2}{(2l+1)}y_l(u_l,\phi_0)\right]\\ &= 0\end{aligned} \tag{6}$$

where

$$y_l(\phi_0,u_l) = \frac{1}{r^{l+1}}\int_0^r r_2^l\phi_0(r_2)u_l(r_2)dr_2 + r^l\int_r^\infty \frac{\phi_0(r_2)u_l(r_2)}{r^{l+1}}dr_2 \tag{7}$$

Phase shift $\eta$ (radians) of a partial wave $l$ is calculated from the asymptotic value of the scattering function.

$$\lim_{r\to\infty} u(r) = \sin\left(kr - l\frac{\pi}{2} + \eta\right). \tag{8}$$

In hybrid theory [6], we replace Eq. (1) by

$$\Psi_L\left(\vec{r}_1,\vec{r}_2\right) = u_L\left(\vec{r}_1\right)\Phi^{pol}\left(\vec{r}_1,\vec{r}_2\right) \pm (1\leftrightarrow 2) + \Phi_L\left(\vec{r}_1,\vec{r}_2\right), \tag{9}$$

where the polarized target function is given in [7] and is defined as

$$\Phi^{pol}\left(\vec{r}_1,\vec{r}_2\right) = \phi_0\left(\vec{r}_2\right) - \frac{\chi(r_1)}{r_1^2}\frac{u_{1s\to p}(r_2)}{r_2}\frac{\cos(\theta_{12})}{\sqrt{\pi Z}}. \tag{10}$$

The cutoff function, instead of $\varepsilon(r_1,r_2) = 1$ for $r_1 > r_2$, is used in the electron-hydrogen scattering calculation [7], and a cutoff function $\chi(r_1)$ given by Shertzer and Temkin [8] of the form

$$\chi_{ST}(r_1) = 1 - e^{-2Zr_1}\left[\frac{(Zr_1)^4}{3} + \frac{4(Zr_1)^3}{3} + 2(Zr_1)^2 + 2Zr_1 + 1\right] \tag{11}$$

is used in this calculation. It can also be of the form

$$\chi(r_1) = \left(1-e^{-\beta r_1}\right)^n, \tag{12}$$

where the exponent $n \geq 3$ and $\beta$, another parameter which is a function of $k$, can be used to optimize the phase shifts. Both cutoffs (11) and (12) are used in calculations on scattering. $\Phi_L(r_1, r_2)$ is a short-range correlation function [6] which can be written using the Euler angle decomposition [9] for all partial waves. This formulism allows the separation of the angular parts and the radial parts consisting of radial coordinates $r_1$, $r_2$, and $r_{12}$. This facilitates writing the equation for radial functions [9]. The function $u_{1s\to p}(r_1)$ in Eq. (10) is given by

$$u_{1s\to p}(r_2) = e^{-Zr_2}\left(\frac{Z}{2}r_2^3 + r_2^2\right) \tag{13}$$

A comparison of results for singlet and triplet phase shifts obtained using different methods is given in **Tables 1** and **2**. Results from most methods agree. A comparison of the singlet and triplet phase shifts obtained by the $R$-matrix and the hybrid theory is given in **Figure 1**. The curves for the two methods cannot be distinguished, showing that accurate result can be obtained using the hybrid theory [6].

The scattering length $a$ is defined by.

$$\lim_{k\to 0} k\cot\eta = -1/a. \tag{14}$$

The scattering length is calculated at a distance $R$, and there is a correction for the long-range polarization [12].

$$a = a(R) - \alpha\left(\frac{1}{R} - \frac{\alpha}{R^2} + \frac{\alpha^2}{3R^3}\right), \tag{15}$$

where $a$ is the true scattering length and $\alpha$ is the polarizability of the hydrogen atom. At $R$ = 117.3088, $^1S$ scattering length $a(R)$ is 5.96554, obtained using $\chi_\beta$. The corrected $^1S$ scattering length is 5.96611. At $R$ = 349.0831, the $^3S$ scattering length is 1.781542, obtained using $\chi_\beta$, and it is 1.76815, after correction for the long-range polarization given by [12]. The $^1S$ and $^3S$ scattering lengths are therefore 5.96611 and

| $k$ | EA[a] | PO[b] | Kohn[c] | Close-coupling[d] | R-matrix[e] | Feshbach method[f] | Hybrid theory[g] |
|---|---|---|---|---|---|---|---|
| 0.1 | 2.396 | 2.583 | 2.553 | 2.491 | 2.550 | 2.55358 | 2.55372 |
| 0.2 | 1.870 | 2.144 | 2.673 | 1.9742 | 2.062 | 2.06678 | 2.06699 |
| 0.3 | 1.508 | 1.750 | 1.6964 | 1.519 | 1.691 | 1.09816 | 1.69853 |
| 0.4 | 1.239 | 1.469 | 1.4146 | 1.257 | 1.410 | 1.41540 | 1.41561 |
| 0.5 | 1.031 | 1.251 | 1.202 | 1.082 | 1.196 | 1.20094 | 1.20112 |
| 0.6 | 0.869 | | 1.041 | | 1.035 | 1.04083 | 1.04110 |
| 0.7 | 0.744 | 0.947 | 0.930 | | 0.925 | 0.93111 | 0.93094 |
| 0.8 | 0.651 | 0.854 | 0.886 | 0.608 | | 0.88718 | 0.88768 |

[a]*Ref. [1].*
[b]*Ref. [7].*
[c]*Ref. [2].*
[d]*Ref. [5].*
[e]*Ref. [10].*
[f]*Ref. [11].*
[g]*Ref. [6].*

**Table 1.**
*Comparison of $^1$S phase shifts obtained in different methods.*

| *k* | EA[a] | PO[b] | Kohn[c] | Close-coupling[d] | R-matrix[e] | Feshbach method[f] | Hybrid theory[g] |
|---|---|---|---|---|---|---|---|
| 0.1 | 2.908 | 2.949 | 2.9388 | 2.9355 | 2.939 | 2.93853 | 2.93856 |
| 0.2 | 2.679 | 2.732 | 2.7171 | 2.715 | 2.717 | 2.71741 | 2.71751 |
| 0.3 | 2.461 | 2.519 | 2.4996 | 2.461 | 2.500 | 2.49975 | 2.49987 |
| 0.4 | 2.257 | 2.320 | 2.2938 | 2.2575 | 2.294 | 2.29408 | 2.29465 |
| 0.5 | 2.070 | 2.133 | 2.1046 | 2.0956 | 2.105 | 2.10454 | 2.10544 |
| 0.6 | 1.901 | | 1.9329 | | 1.933 | 1.93272 | 1.93322 |
| 0.7 | 1.749 | 1.815 | 1.7797 | | 1.780 | 1.77950 | 1.77998 |
| 0.8 | 1.614 | 1.682 | 1.643 | 1.616 | | 1.64379 | 1.64425 |

[a]*Ref. [1].*
[b]*Ref. [7].*
[c]*Ref. [2].*
[d]*Ref. [5].*
[e]*Ref. [10].*
[f]*Ref. [11].*
[g]*Ref. [6].*

**Table 2.**
*Comparison of* $^3$S *phase shifts obtained in different methods.*

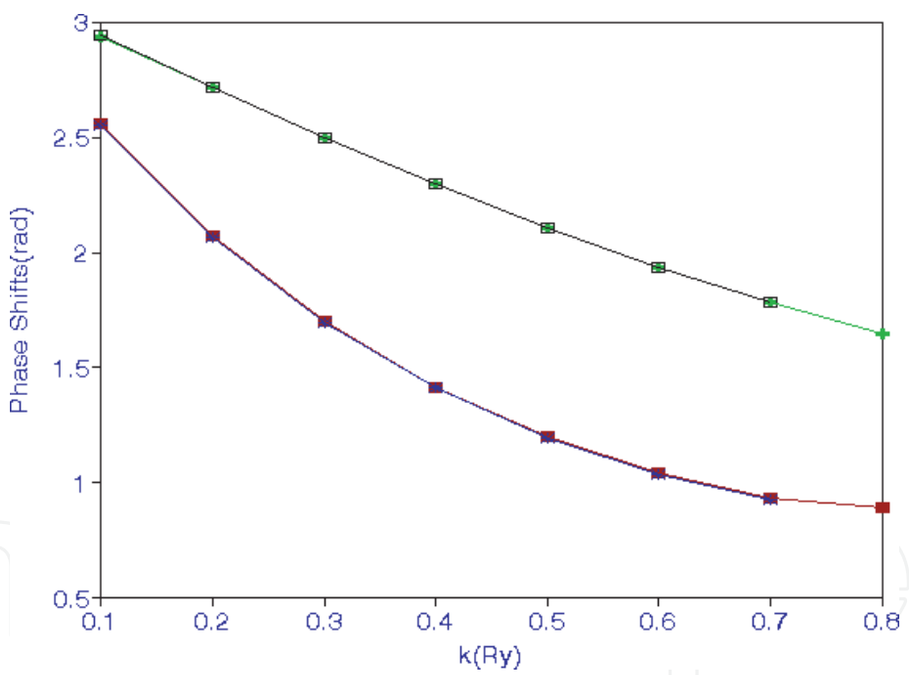


**Figure 1.**
*The upper represents singlet phase shifts obtained in the hybrid and* R*-matrix theories. The two curves cannot be distinguished. Similarly, the lower curves represent triplet phase shifts obtained in the two theories.*

1.76815, which agree with those calculated by Schwartz [2], using the Kohn variational method. In this method, scattering lengths have upper bounds, while phase shifts do not have any bounds in this method (Kohn variational method). Similar calculations for the phase shifts for e-$He^+$ and e-$Li^{2+}$ have been carried out in Ref. [13].

Resonance parameters in two-electron systems have been calculated using various approaches. Among them are the stabilization method, the complex-rotation method, the close-coupling method, and the Feshbach projection-operator formalism. In the hybrid theory, phase shifts have been calculated in the resonance region [13] and are fitted to the Breit-Wigner form

$$\eta_{calc.}(E) = \eta_0 + AE + \tan^{-1}\frac{0.5\Gamma}{(E_R - E)}. \quad (16)$$

In the above equation, $E = k^2$ is the incident energy, $\eta_{calc.}$ are the calculated phase shifts, and $\eta_0$, $A$, $\Gamma$, and $E_R$ are the fitting parameters. $E_R$ and $\Gamma$ represent the resonance position and resonance width, respectively. We find that in the hybrid theory, the He singlet resonance is at $E_R$ = 57.8481 eV with respect to the ground state of He and $\Gamma$ = 0.1233 eV. They agree well with $E_R$ = 57.8435 eV and $\Gamma$ = 0.125 eV obtained using the Feshbach projection-operator formalism [14]. A similar calculation [13] has been carried out for $Li^{2+}$ resonance parameters. The resonance parameters agree with those obtained in [14].

P-wave phase shifts have been calculated for scattering of electrons from $He^+$ and $Li^{2+}$ in Ref. [15] and in Ref. [16], respectively. Singlet P and triplet P phase shifts are shown in **Table 3** for e + $He^+$ and for e + $Li^{2+}$ scattering. Phase shifts for e + $He^+$ agree well with those obtained by Oza [17] using the close-coupling approximation. Phase shifts for e + $Li^{2+}$ agree with those obtained by Gien [18] using the Harris-Nesbet method.

| $k$ | $^1P$ | $^3P$ | $^1P$ | $^3P$ |
|---|---|---|---|---|
| | e + $He^+$ [15] | | e + $Li^{2+}$ [16] | |
| 0.1 | −0.038308 | 0.21516 | −0.049083 | 0.16323 |
| 0.2 | −0.038956 | 0.21683 | −0.048990 | 0.16334 |
| 0.3 | −0.039873 | 0.21945 | −0.048934 | 0.16341 |
| 0.4 | −0.040902 | 0.22283 | −0.48823 | 0.16351 |
| 0.5 | −0.041469 | 0.22662 | −0.048565 | 0.16360 |
| 0.6 | −0.041641 | 0.23088 | −0.048306 | 0.16379 |
| 0.7 | −0.041438 | 0.23417 | −0.047972 | 0.16382 |
| 0.8 | −0.039927 | 0.23753 | −0.047547 | 0.16374 |
| 1.0 | −0.037132 | 0.24205 | −0.045966 | 0.16409 |
| 1.1 | −0.035430 | 0.24323 | −0.045029 | 0.16399 |
| 1.3 | −0.026419 | 0.24370 | −0.042670 | 0.16345 |
| 1.4 | −0.020773 | | −0.041251 | 0.16299 |
| 1.6 | | | −0.037973 | 0.16158 |

**Table 3.**
*Phase shifts (radians) for e + $He^+$ and e + $Li^{2+}$ scattering.*

## 3. Photoabsorption

Photodetachment and photoionization are required to calculate radiative-attachment cross sections. The recombination rates are required to calculate the ionization balance in astrophysical plasmas. Cross sections for bound-free transitions of $H^-$ are required to account for the absorption in the solar atmosphere [19]. The opacity in the sun is due to photodetachment and free-free absorption of the radiation:

$$h\nu + H^- \rightarrow H + e, \quad (17)$$

$$h\nu + e + H \rightarrow e + H, \tag{18}$$

In the first process, after absorption of the radiation by the bound electron, it becomes a free electron in the final state, while in the free-free transition, the electron is in the continuum state in the initial state as well as in the final state. It is possible to have the following reactions which help molecular formation:

$$\begin{aligned} e + H &\rightarrow H^- + h\nu \\ H^- + H &\rightarrow H_2 + e. \end{aligned} \tag{19}$$

The photoabsorption cross section in length form and in units of $a_o^2$ for the transition from the initial states $I$ to the final state $f$ is given by

$$\sigma\left(a_0^2\right) = 4\pi\alpha\omega|<\Psi_f|z_1 + z_2|\Phi_i>|^2. \tag{20}$$

In the above equation, $\alpha$ is the fine-structure constant, $k$ is the momentum of the outgoing electron, $\omega = I + k^2$ is the energy of the incident photon, and $I$ is the ionization potential of the system absorbing the photon. Photoabsorption cross sections for $H^-$, He, and $Li^+$ are given in [16] and in **Table 4**. The correlated wave functions for $H^-$, He, and $Li^+$ are of Hylleraas form having terms 364, 220, and 165, respectively. A Hyllerraas wave function is given by

$$\Psi(r_1, r_2, r_{12}) = \sum C_{lmn}\left[e^{-\gamma r_1 - \delta r_2} r_1^l r_2^m r_{12} \pm (1 \leftrightarrow 2)\right]. \tag{21}$$

In Eq. (21), $C$'s are the linear parameters, while $\gamma$ and $\delta$ are nonlinear parameters, and $r_{12} = |\vec{r}_1 - \vec{r}_2|$. Ohmura and Ohmura [20] have calculated the photodetachment cross section of $H^-$, using the effective range theory and the loosely bound structure of hydrogen ion. These cross sections are shown in **Figure 2**. It should be noticed that with the outgoing energy of the electron going to zero, the cross section goes to zero when the remaining system is neutral and is finite when the remaining system is an ion [16].

A comparison of the cross sections of the ground state of He with those obtained in the $R$-matrix [21] is shown in **Figure 3**. The agreement is very good except at $k = 0.6$ where the $R$-matrix result is slightly lower. It seems that the cross section has not been calculated accurately at this $k$. The precision measurements of the cross sections of photoionization of He by Samson et al. [22] are also shown in **Figure 3**,

| $k$ | $H^-$ | He | $Li^+$ |
|---|---|---|---|
| 0.1 | 15.3024 | 7.3300 | |
| 0.2 | 38.5443 | 7.1544 | 2.5677 |
| 0.3 | 35.2318 | 6.8716 | 2.5231 |
| 0.4 | 24.4774 | 6.4951 | 2.4373 |
| 0.5 | 16.0858 | 6.0461 | 2.3870 |
| 0.6 | 10.7410 | 5.5925 | 2.2988 |
| 0.7 | 7.4862 | 5.0120 | 2.0005 |
| 0.8 | 5.6512 | 4.4740 | 2.0925 |
| 0.9 | | 3.9296 | 1.9792 |

**Table 4.**
*Photoabsorption cross (Mb) for the ground state of $H^-$, He, and $Li^+$.*

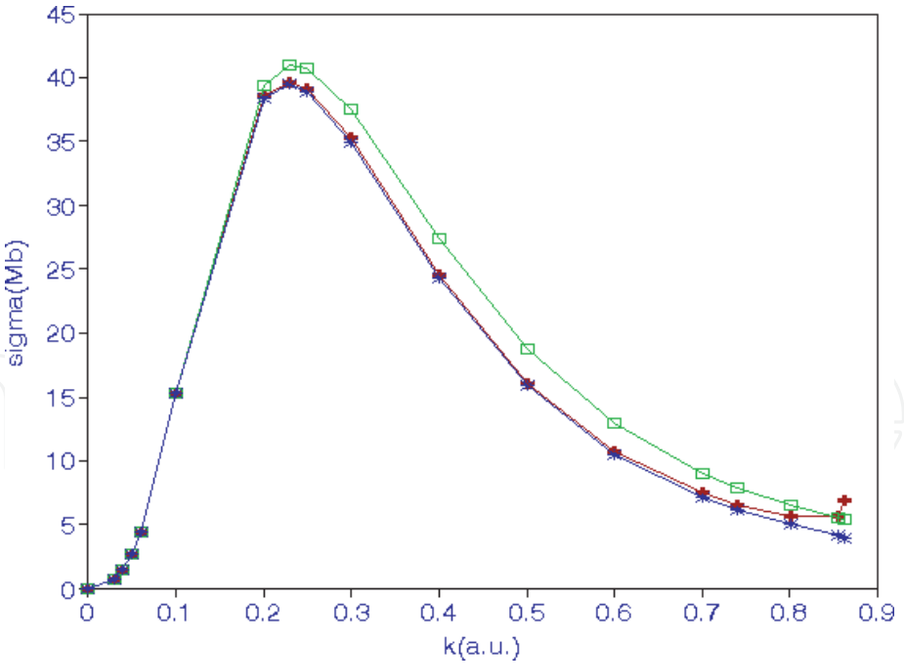


**Figure 2.**
*Photodetachment of a hydrogen ion. The lowest curve is obtained when only the long-range correlations are included; the middle curve is obtained when the short-range and long-range correlations are also included. The top curve is obtained using Ohmura and Ohmura formulation.*

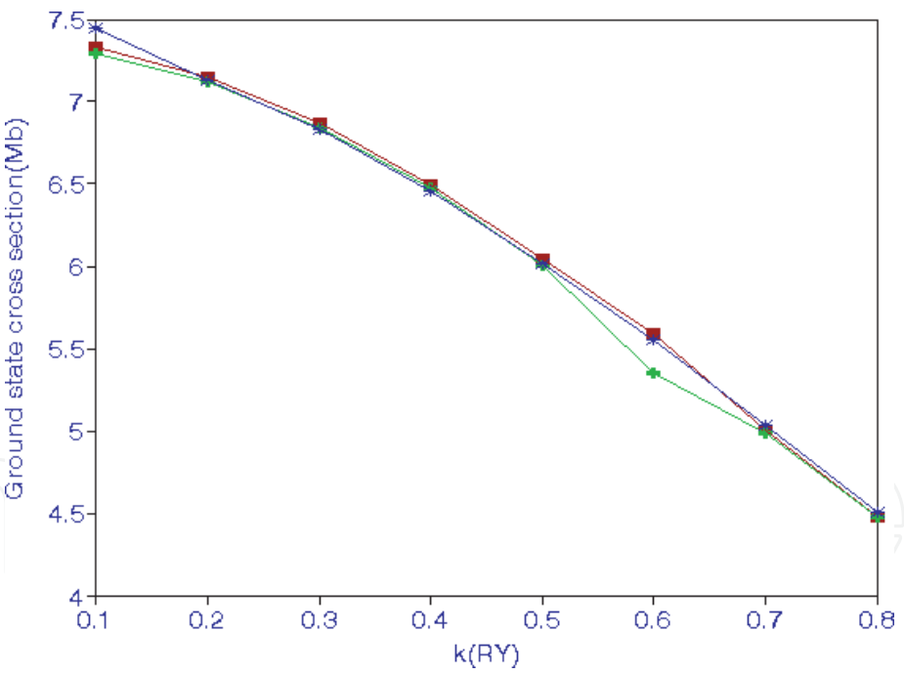


**Figure 3.**
*The upper curve represents photoionization cross sections (Mb) for the ground state of He in the hybrid theory, while the lower represents cross sections obtained in* R*-matrix calculations. The curve starting at the top left represents experimental results of Samson et al. [22].*

showing that the agreement with the cross sections obtained using the hybrid theory is very good.

Similarly, cross sections have been calculated in [16] for the (1s2s) $^1S$ and (1s2s) $^3S$ metastable states of He and $Li^+$. The number of Hylleraas terms used are 455 and 364 for He singlet and triplet states, respectively. For $Li^+$, 120 and 220 terms are used for the singlet and triplet states, respectively. These cross sections are comparable to those obtained for the ground state. A comparison of photoionization cross

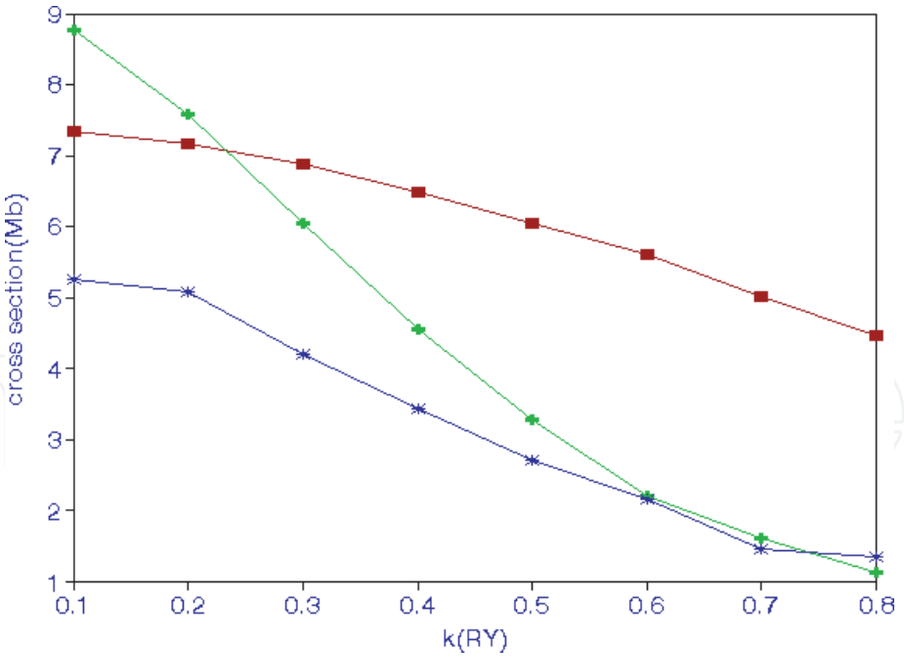


**Figure 4.**
*Photoionization cross section for the ground state (middle curve from the right), for the (1s2s) singlet* S *state (top curve), and for the (1s2s) triplet* S *state (lower curve) of the He atom.*

sections of the ground state, metastable states singlet *S*, and triplet *S* is shown in **Figure 4**. The cross section for the singlet (1s2s) state is highest at $k = 0.1$, and then the cross sections decrease rapidly.

## 4. Excitation

Excitation of the 1*S* state of atomic hydrogen to the 2*S* state has been calculated using the hybrid theory in the distorted-wave approximation [23]. The total excitation cross section is written in the form

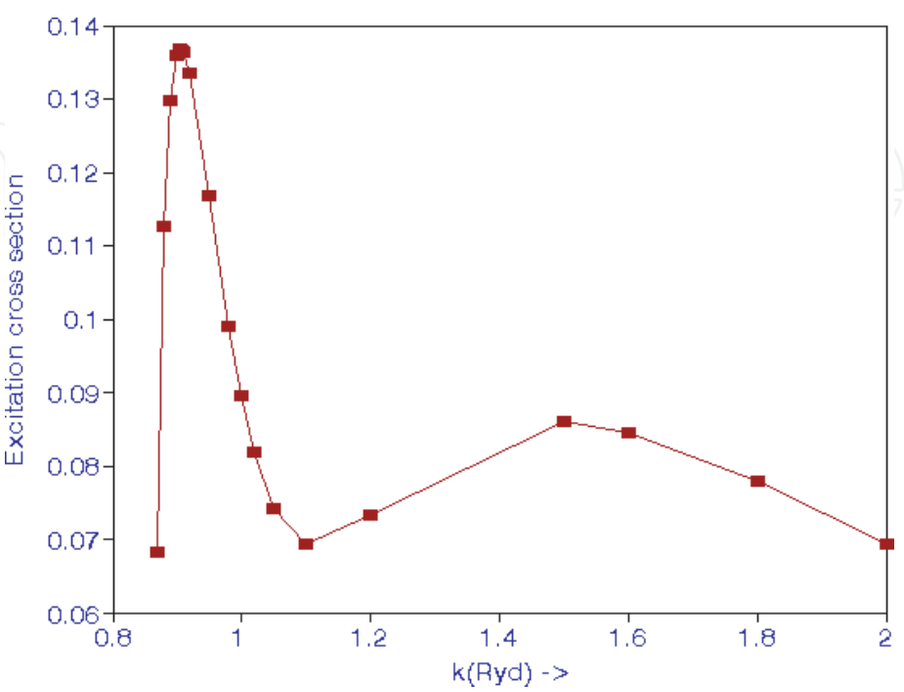


**Figure 5.**
*Cross section (Mb) for exciting the* 1S *state to* 2S *state of atomic hydrogen by electron impact.*

| $k$ | He | | $Li^+$ | |
|---|---|---|---|---|
| | $(1s2s)^1S$ | $(1s2s)^3S$ | $(1s2s)^1S$ | $(1s2s)^3S$ |
| 0.1 | 8.7724 | 5.2629 | 2.4335 | 2.9889 |
| 0.2 | 7.5894 | 5.0795 | 2.3742 | 2.8570 |
| 0.3 | 6.0523 | 4.2004 | 2.2287 | 2.6434 |
| 0.4 | 4.5403 | 3.4403 | | 2.3733 |
| 0.5 | 3.2766 | 2.7189 | | 2.0865 |
| 0.6 | 2.2123 | 2.1531 | | 1.7962 |
| 0.7 | 1.6047 | 1.4564 | | 1.5182 |
| 0.8 | 1.1230 | 1.3539 | | 1.2627 |

**Table 5.**
*Photoionization cross sections (Mb) for the metastable states of He and $Li^+$ with the outgoing electron with momentum* k.

$$\sigma = \frac{k_f}{k_i}\int |T_{fi}|^2 d\Omega. \tag{22}$$

In the above equation, $k_i$ and $k_f$ are the incident and final momenta, and $T_{fi}$ is the matrix element for the excitation of the initial state $i$ to the final state $f$ and is given by

$$T_{fi} = -(1/4\pi) < \Psi_f | V | \Psi_i > . \tag{23}$$

$$V = -\frac{2Z}{r_1} + \frac{2}{r_{12}}. \tag{24}$$

$Z$ is the nuclear charge, and $r_1$ and $r_2$ indicate the position of the incident and target electron, respectively. The excitation cross sections at $k$(Ry) = 0.8–2 are shown in **Figure 5**. There is a maximum at $k$ = 0.907 and another at $k$ = 1.50 (**Table 5**).

## 5. Recombination

Recombination rate coefficients for a process like that indicated in Eq. (17) have been calculated in Ref. [16] for the ground states as well as for the metastable states. The attachment cross section $\sigma_a$ is given by

$$\sigma_a = \left(\frac{h\nu}{cp_e}\right)^2 \frac{g(f)}{g(i)}\sigma. \tag{25}$$

The above relation between the photodetachment and photoionization follows from the principle of detailed balance, where $g(i)$ and $g(f)$ are the weight factors for the initial and final states, and $p_e = k$ is the electron momentum. The attachment cross sections are in general smaller than the photoabsorption cross sections. Recombination rate coefficients, averaged over the Maxwellian velocity distribution, are given in **Table 6** for $H^-$, He, and $Li^+$ for a temperature range from 1000 to 40,000 K.

Elastic $P$-wave scattering from e- $Be^{3+}$, $C^{5+}$, and $O^{7+}$ and photoionization in two-electron systems have been carried out. Phase shifts and photoionization cross sections are given in [24] for the ground as well as metastable states. In order to

| $T$ | $\alpha_R(T) \times 10^{15}$, $H^-$ | $\alpha_{(R)}(T) \times 10^{13}$, He | $\alpha_R(T) \times 10^{13}$, $Li^+$ |
|---|---|---|---|
| 1000 | 0.99 | 2.50 | 0.12 |
| 2000 | 1.28 | 2.39 | 1.04 |
| 5000 | 2.40 | 1.87 | 2.62 |
| 7000 | 2.82 | 1.66 | 2.92 |
| 10,000 | 3.20 | 1.45 | 3.03 |
| 12,000 | 3.37 | 1.35 | 3.02 |
| 15,000 | 3.56 | 1.23 | 2.95 |
| 17,000 | 3.65 | 1.17 | 2.89 |
| 20,000 | 3.75 | 1.10 | 2.79 |
| 22,000 | 3.79 | 1.05 | 2.73 |
| 25,000 | 3.83 | 0.99 | 2.63 |
| 30,000 | 3.83 | 0.92 | 2.49 |
| 35,000 | 3.77 | 0.87 | 2.36 |
| 40,000 | 3.63 | 0.82 | 2.25 |

**Table 6.**
*Recombination rate coefficients ($cm^3/s$) for ($1s^2$) $^1$S states of $H^-$, He, and $Li^+$.*

| $k$ | $^1D$, e-H | $^3D$, e-H | $^1D$, e-$He^+$ | $^3D$, e-$He^+$ | $^1D$, e-$Li^{2+}$ | $^3D$, e-$Li^{2+}$ |
|---|---|---|---|---|---|---|
| 0.1 | 1.3193 (−3) | 1.3217 (−3) | 5.9268 (−3) | 8.5133 (−3) | 3.0363 (−3) | 8.2703 (−3) |
| 0.2 | 5.0217 (−3) | 5.0835 (−3) | 6.1299 (−3) | 9.0331 (−3) | 3.0585 (−3) | 8.4642 (−3) |
| 0.3 | 1.0531 (−2) | 1.0898 (−2) | 6.4446 (−3) | 9.8834 (−3) | 3.0508 (−3) | 8.7011 (−3) |
| 0.4 | 1.7250 (−2) | 1.8401 (−2) | 6.8511 (−3) | 1.1044 (−2) | 3.0776 (−3) | 9.0700 (−2) |
| 0.5 | 2.4675 (−2) | 2.7204 (−2) | 7.3028 (−3) | 1.2473 (–2) | 3.0782 (−3) | 9.5041 (−2) |
| 0.6 | 3.2495 (−2) | 3.6934 (−2) | 7.7904 (−3) | 1.4152 (−2) | 3.0608 (−3) | 1.0009 (−2) |
| 0.7 | 4.0544 (−2) | 4.7286 (−2) | 8.3087 (−3) | 1.6066 (−2) | 3.0831 (−3) | 1.0622 (−2) |
| 0.8 | 4.8620 (−2) | 5.7990 (−2) | 8.8420 (−3) | 1.8172 (−2) | 3.1396 (−3) | 1.1380 (−2) |
| 0.9 | 5.6532 (−2) | 6.8791 (−2) | 9.3860 (−3) | 2.0439 (−2) | 3.1537 (−3) | 1.2151 (−2) |

**Table 7.**
*D-wave phase shifts (radians) for e-H, e-$He^+$, and e-$Li^{2+}$.*

calculate photoionization cross sections from $P$-state of an atom, both $S$-wave and $D$-wave continuum functions are needed. We give a few phase shifts for $^1D$ and $^3D$ in **Table 7** for scattering from H, $He^+$, and $Li^{2+}$.

## 6. Laser fields

Scattering cross sections have also been calculated in the presence of laser fields [25]. A strong suppression in the laser-assisted cross sections is noted when compared to cross sections in the field-free situation. Further, scattering cross sections have also been calculated in the presence of Debye potential [26], in addition to the laser field.

## 7. Positron-hydrogen scattering

Dirac in 1928, combining the ideas of relativity and quantum mechanics, formulated the well-known relativistic wave equation and predicted an antiparticle of the electron of spin ħ/2. At that time only protons and electrons were known. He thought that the antiparticle must be proton. Hermann Weyl showed from symmetry considerations that the antiparticle must have the same mass as an electron. There are many other examples where symmetry played an important role, e.g., Newton's third law of motion (for every action there is an equal and opposite reaction) and Faraday's laws of electricity and magnetism (electric currents generate magnetic fields, and magnetic fields generate electric currents). Symmetry laws have some profound implications as shown by Emmy Noether in 1918 that every symmetry in the action is related to a conservation law [27].

Positrons, produced by cosmic rays in a cloud chamber, were detected by Anderson [28] in 1932. Positrons can form positronium atoms which annihilate, giving 511 KeV line with a width of 1.6 keV. This line has been observed from the center of the galaxy. Positrons have become very useful to scan the human brain (PET scans). They have been used to probe the Fermi surfaces, and the annihilation of positronium atoms in metals has been used to detect defects in metals.

Calculations of positron-hydrogen scattering should be simpler than the electron-hydrogen scattering because of the absence of the exchange between electrons and positrons. However, the complications arise due to the possibility of positronium atom formation. In electron-hydrogen system, the two electrons are on either side of the proton because of the repulsion between two electrons. However, because of the attraction between a positron and an electron, both the positron and the bound electron tend to be on the same side of the proton. This configuration shows that the correlations are more important in the case of a positron incident on a hydrogen atom. In 1971, we [29] carried out calculations using the projection-operator formulism of Feshbach [4] and using generalized Hylleraas-type functions:

$$\Psi(r_1, r_2, r_{12}) = e^{-\gamma r_1 - \delta r_2 - \alpha r_{12}} \sum_{lmn} C_{lmn} r_1^l r_2^m r_{12}^n. \tag{26}$$

Nonlinear parameters are $\gamma$, $\delta$, and $\alpha$ and $C$'s are the linear coefficients. The results obtained agree with those obtained by Schwartz [2]. However, the long-range correlations could not be taken into account in [29] at the same time and had to be added separately, with the result that the final phase shifts ceased to have any

| $k$ | Hybrid theory [30] | Bhatia et al. [29] | Schwarz [2] | Hybrid theory [31] | Bhatia et al. [32] | Armstrong [33] |
|---|---|---|---|---|---|---|
| | | *S*-wave | | | *P*-wave | |
| 0.1 | 0.14918 | 0.1483 | 0.151 | 0.008871 | 0.00876 | 0.008 |
| 0.2 | 0.18803 | 0.1877 | 0.188 | 0.032778 | 0.03251 | 0.032 |
| 0.3 | 0.16831 | 0.1677 | 0.168 | 0.06964 | 0.6556 | 0.064 |
| 0.4 | 0.12083 | 0.1201 | 0.120 | 0.10047 | 0.10005 | 0.099 |
| 0.5 | 0.06278 | 0.0624 | 0.062 | 0.13064 | 0.13027 | 0.130 |
| 0.6 | 0.00903 | 0.0039 | 0.007 | 0.15458 | 0.15410 | 0.153 |
| 0.7 | 0–0.04253 | −0.0512 | −0.54 | 0.17806 | 0.17742 | 0.175 |

**Table 8.**
*Comparison of* S*-wave and* P*-wave phase shifts obtained in the hybrid theory with results obtained earlier.*

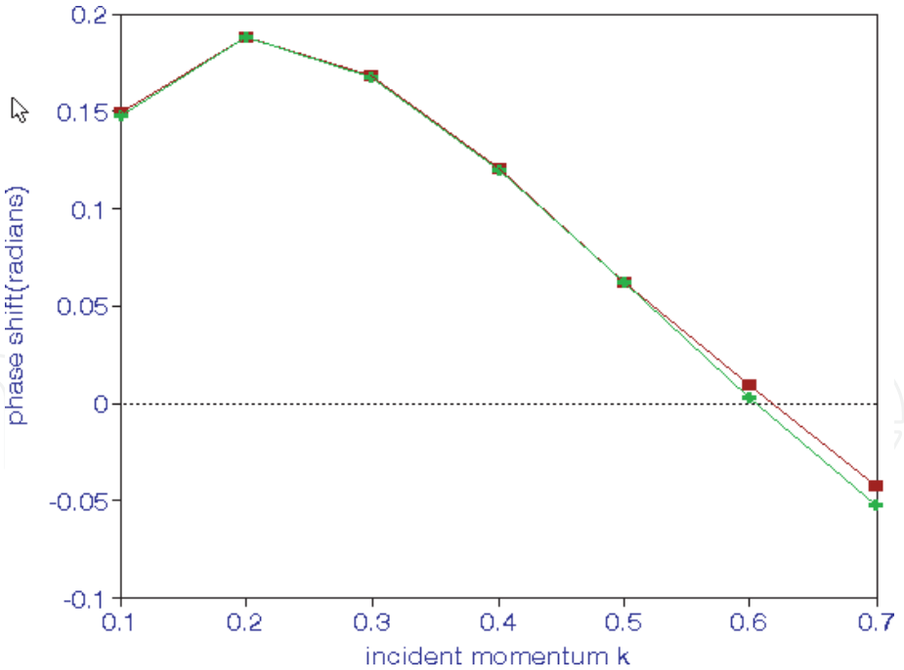


**Figure 6.**
*The upper curve represents phase shifts obtained using the hybrid theory, and the lower curve represents phase shifts obtained using the Feshbach formalism.*

bounds. In the hybrid theory, as indicated earlier, both short-range and long-range correlations can be taken into account at the same time. It should be noted that in the case of positrons, the sign before the second term in Eq. (10) is plus instead of minus, as in the case of electrons. The phase shifts obtained in two approaches are given in **Table 8**. We used 84 terms in the Hylleraas wave function previously, and improved results are obtained now with shorter expansions [30] as indicated in the table. A comparison of the results obtained with different approaches is shown in **Figure 6**. Using a fewer number of terms, higher phase shifts have been obtained in the hybrid theory [30]. P-wave shifts have been calculated in the hybrid theory [31] and are compared with those using the Feshbach projection-operator formalism [32] and with those obtained by Armstrong [33].

## 8. $Z_{eff}$

The incident positron can annihilate the atomic electron with the emission of two gamma rays. The cross section for this process has been given by Ferrell [34]:

$$\sigma_a\left(\pi a_0^2\right) = Z_{eff}\alpha^3 k^{-1} \tag{27}$$

where $\alpha$ is the fine-structure constant and

$$Z_{eff} = \int d\vec{r}_1 d\vec{r}_2 \left|\Psi\left(\vec{r}_1, \vec{r}_2\right)\right|^2 \delta\left(\vec{r}_1, \vec{r}_2\right). \tag{28}$$

$Z_{eff}$ for partial waves $l$ = 0 and 1, obtained in [31, 32], is given in **Table 9** along with the contribution from $l > 1$. For higher partial waves, $Z_{eff}$ is given by

$$Z_{eff}(l>1) = \frac{k^2}{1+k^2} + \frac{6}{k^2}\left[\frac{1}{k^2}\ln\left(1+k^2\right) - \frac{1+0.5k^2}{1+k^2}\right]. \tag{29}$$

| $k$ | $Z_{eff}$ ($l = 0$) | $Z_{eff}$ ($l = 1$) | $Z_{eff}$ ($l > 1$) | Total |
|---|---|---|---|---|
| 0.1 | 7.363 | 0.022 | <0.001 | 7.385 |
| 0.2 | 5.538 | 0.90 | 0.001 | 5.629 |
| 0.3 | 4.184 | 0.187 | 0.004 | 4.375 |
| 0.4 | 3.327 | 0.294 | 0.010 | 3.631 |
| 0.5 | 2.730 | 0.390 | 0.022 | 3.142 |
| 0.6 | 2.279 | 0.464 | 0.039 | 2.782 |
| 0.7 | 1.850 | 0.528 | 0.063 | 2.541 |

**Table 9.**
*$Z_{eff}$ for positron-hydrogen scattering.*

## 9. Positronium formation

Positronium, the bound state of an electron and a positron, was predicted by Mohorovicic [35] in connection with the spectra of nebulae. Positronium (Ps) formation takes place when the incident positron captures the bound electron of the hydrogen atom:

$$e^+ + H(1s) \rightarrow Ps + P. \tag{30}$$

Cross sections for the positronium formation are given in **Table 10** and are compared with those obtained by Khan and Ghosh [36] and Humberston [37].

| $k^2$ | Hybrid theory | Khan and Ghosh [36] | Humberston [37] |
|---|---|---|---|
| 0.5041 | 0.0066228 | 0.009037 | 0.0041 |
| 0.5476 | 0.018783 | | |
| 0.5625 | 0.0.20249 | 0.024795 | 0.0044 |
| 0.64 | 0.022566 | 0.0248 | 0.0049 |
| 0.6724 | 0.022350 | | |
| 0.7225 | 0.21456 | 0.021164 | 0.0058 |
| 0.75 | 0.020835 | 0.019707 | |
| 0.81 | 0.19256 | | |
| 0.9025 | 0.016760 | | |
| 1.00 | 0.014327 | | |

**Table 10.**
*Cross sections $(\pi a_o^2)$ for positronium formation obtained in hybrid theory and in comparison with those obtained by Khan and Ghosh [36] and Humberston [37].*

## 10. Photodetachment of positronium ion ($Ps^-$)

Photodetachment has been discussed above already. Following the work of Ohmura and Ohmura [20], Bhatia and Drachman [38] calculated cross sections (in the length and velocity form) for photodetachment of $Ps^-$. Their result in length and velocity form is

$$\sigma = \left(1.32 \times 10^{-18}\text{cm}^2\right) \frac{k^3}{\left(k^2 + \gamma^2\right)^3}. \tag{31}$$

The electron affinity is $\frac{3\gamma^2}{2}$, where $\gamma = 0.12651775$ [39] and $k$ is the momentum of the outgoing electron. These cross sections are much larger than that for the photodetachment of the negative hydrogen ion.

Lyman-α radiation ($2P \rightarrow 1S$) at 1216 Å has been seen from astrophysical sources and the sun. It has been observed from Voyager measurements [40]. Similarly, Lyman-α radiation ($2P \rightarrow 1S$) at 2416 Å is expected when in the photodetachment of $Ps^-$, the remaining positronium is left in the $2P$ state. Following Ohmura and Ohmura [20], photodetachment cross sections have been calculated when the remaining atom is in $2p$, $3p$, $4p$, $5p$, $6p$, and $7p$ states [41].

$$\begin{aligned} o(2p) &= 164.492C(k) \\ \sigma(3p) &= 26.3782C(k) \\ \sigma(4p) &= 9.1664C(k) \\ \sigma(5p) &= 4.3038C(k) \\ \sigma(6p) &= 2.3764C(k) \\ \sigma(7p) &= 0.2675C(k) \end{aligned} \tag{32}$$

These cross sections are given in **Figure 7** for various photon energies.

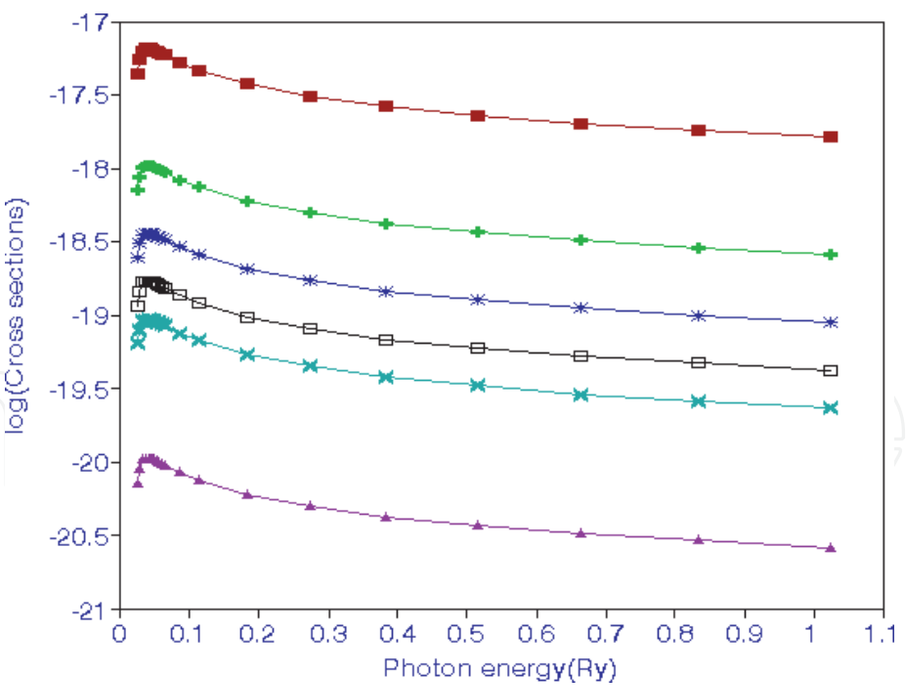


**Figure 7.**
*The upper most curve represents photodetachment cross sections for* n = 2 *on* $\log_{10}$ *scale. The curves below it are for n = 3, 4, 5, 6, and 7.*

## 11. Binding energies

Positrons do not bind with hydrogen atoms. However, they do bind with various atoms as has been shown by Mitroy et al. [42]. The binding energies are given in **Table 11**.

| He ($^3S$) | Li | Be | Na | Mg |
|---|---|---|---|---|
| 0.0011848 | 0.004954 | 0.006294 | 0.000946 | 0.031224 |
| **Ca** | **Sr** | **Cu** | **Au** | **Cd** |
| 0.03300 | 0.0201 | 0.011194 | 0.011664 | 0.01220 |

**Table 11.**
*Binding energies (Ry) of positrons with various atoms.*

## 12. Resonances

Resonances formed in the scattering of electrons from atoms are very common. However, they are not that common in positron-target systems. The first successful prediction of $S$-wave Feshbach resonance in positron-hydrogen system is by Doolen et al. [43], who, using the complex-rotation method, obtained the position $-0.2573741$ and for width 0.0000677 Ry. In this method

$$r \rightarrow re^{-i\theta}, T \rightarrow Te^{-2i\theta}, \text{and } V \rightarrow Ve^{-i\theta} \text{ and } H = T + V. \tag{33}$$

Eigenvalues are complex now. The real part gives position of the resonance, and the imaginary part gives its half width.

A number of Feshbach and shape resonances in $Ps^-$ have been calculated by using the complex-rotation method. Parameters of a $^1P$ shape resonance above $n = 2$ have been calculated by Bhatia and Ho [44]. They obtained $-0.06217$ and 0.000225 Ry for the position and width of the resonance. These results have been confirmed experimentally by Michishio et al. [45].

## 13. Antihydrogen formation

Antihydrogen can be formed in the collision of Ps with antiproton

$$Ps + \overline{p} \rightarrow \overline{H} + e. \tag{34}$$

In the above equation, $\overline{p}$ represents antiproton and $\overline{H}$ represents antihydrogen. According to the time reversal invariance, the above reaction is related to

$$Ps + p \rightarrow H + e^+. \tag{35}$$

From this reaction, the positronium formation cross sections are known from positron-hydrogen scattering. This implies that the cross section for antihydrogen is related to the cross section for Ps formation:

$$\sigma_{\overline{H}} = \left(\frac{k_{e^+}}{k_{Ps}}\right)^2 \sigma_{Ps}. \tag{36}$$

$k_{e^+}$ and $k_{\mathrm{Ps}}$ are momenta of positron and positronium. Humberston et al.

[46] have calculated cross sections for the formation of antihydrogen in reaction (34). It is possible to form antihydrogen by radiative recombination or three-body recombination:

$$e^+ + \overline{p} \rightarrow \overline{H} + h\nu. \tag{37}$$

$$e^+ + e^+ + \overline{p} \rightarrow \overline{H} + e^+. \tag{38}$$

If the antihydrogen is formed in the excited state, then it can decay to the lower states. It would then be possible to verify if the quantum mechanics principles are the same in the antimatter universe. It is thought that gravitational interactions should be the same between matter and antimatter and between antimatter and antimatter. However, there is no experimental confirmation up to now.

## 14. High-energy cross sections

At high energies, only static potential remains. Therefore, according to the first Born approximation, total cross sections for $e^-$-He and $e^+$-He should be the same. This fact has been verified experimentally by Kauppila et al. [47], and their results are shown in **Table 12**. We see that as the incident energy increases, cross sections tend to be equal.

| Energy (eV) | $e^-$-He | $e^+$-He |
|---|---|---|
| 50 | 1.27 | 1.97 |
| 100 | 1.16 | 1.26 |
| 150 | 0.967 | 0.987 |
| 200 | 0.796 | 0.812 |
| 300 | 0.614 | 0.612 |
| 500 | 0.437 | 0.434 |
| 600 | 0.371 | 0.381 |

**Table 12.**
*Cross sections measured by Kauppila et al. [47] for $e^-$-He and $e^+$-He scattering.*

## 15. Total positron-hydrogen cross sections

Total cross sections for positron scattering from hydrogen atoms have been measured by Zhou et al. [48] and have been calculated by Walters [49] using the close-coupling approximation and also by Gien [50] using the modified Glauber approximation. Their results are given in **Table 13**. They are fairly close to the experimental results.

| *E* (eV) | Ref. [49] | Ref. [50][a] |
|---|---|---|
| 54.4 | 3.02 | 2.85 |
| 100 | 2.24 | 2.00 |
| 200 | 1.33 | 1.24 |
| 300 | 9.69 (−1) | 8.73 (−1) |

[a]*Cross sections have been interpolated from those given in Ref. [50].*

**Table 13.**
*Positron-hydrogen total cross sections.*

## 16. Threshold laws

When the incident electron or positron has just enough energy to ionize the hydrogen atom, how do the cross sections behave? Wannier [51], using classical methods and supposing the two electrons emerge opposite to each other, showed that $\sigma \propto E^{1.127}$, where $E$ *i*s the excess energy. As indicated earlier in the positron-hydrogen scattering, positron and electron tend to be on the same side of the nucleus. This shows the cross section at threshold cannot be the same for positrons and electrons. The threshold behavior of the positron impact on hydrogen has been analyzed by Klar [52]. He finds that at threshold, $\sigma \propto E^{2.650}$.

Wigner [53] has emphasized the importance of long-range forces near the threshold which have been included in these calculations (hybrid theory). At the threshold, the cross section for exciting the 1*S* state of hydrogen atom to the 2*S* state is proportional to $\left(\ln k_f\right)^{-2}$ [54].

## 17. Conclusions

In this chapter, we have discussed various interactions of electrons and positrons with atoms, ions, and radiation fields. There are various approximations and theories to calculate scattering functions. Theories which provide variational bounds on the calculated phase shifts are preferable because improved results can be obtained when the number of functions in the closed channels is increased. Such theories are the close-coupling, *R*-matrix, and hybrid theory. It should be possible to formulate the hybrid theory for more complicated systems.

The continuum functions obtained using the hybrid theory have been used to calculate photoabsorption cross sections, obtaining results which agree with definitive results obtained using other methods and experiments. Such cross sections are needed to study the opacity in the sun. The resonances play an important role when they are included in the calculations of excitation cross sections, which are important to infer temperatures and densities of solar and astrophysical plasmas.

When Feshbach projection-operator formalism [4] is used to calculate resonance position, $E = \varepsilon + \Delta$, where $\Delta$, the shift in the resonance position due to its coupling with the continuum, has to be calculated separately [14]. However, in the hybrid theory, the calculated position includes this correction. This is an advantage since the calculation of the shift is nontrivial.

We have indicated that in addition to obtaining accurate phase shifts for positron scattering from a hydrogen atom, we have described calculations of annihilation, positronium, and antihydrogen formation. We have discussed resonances in a positron-hydrogen system. We have discussed photodetachment of a positronium ion and a possibility of observing Lyman-α radiation from a positronium atom when the final state is the 2*p* state.

IntechOpen

## Author details

Anand K. Bhatia
NASA/Goddard Space Flight Center, United States

*Address all correspondence to: anand.k.bhatia@nasa.gov

## References

[1] Morse PM, Allis WP. The effect of exchange on the scattering of slow electrons from atoms. Physics Review. 1933;**44**:269

[2] Schwartz C. Electron scattering from hydrogen. Physics Review. 1961;**124**: 1468

[3] Temkin A. A note on scattering of electrons from atomic hydrogen. Physics Review. 1959;**116**:358

[4] Feshbach H. A unified theory of nuclear reactions II. Annals of Physics. 1962;**19**:287

[5] Burke PG, Smith K. The low-energy scattering of electrons and positrons by hydrogen atoms. Reviews of Modern Physics. 1962;**34**:458

[6] Bhatia AK. Hybrid theory of electron-hydrogen scattering. Physical Review A. 2007;**75**:032713

[7] Temkin A, Lamkin JC. Application of the method of polarized orbitals to the scattering of electrons from hydrogen. Physics Review. 1961;**121**:788

[8] Shertzer J, Temkin A. Direct calculation of the scattering amplitude without partial-wave analysis III. Inclusion of correlation effects. Physical Review A. 2006;**74**:052701

[9] Bhatia AK, Temkin A. Symmetric euler-angle decomposition of the two-electron fixed – nucleus problem. Reviews of Modern Physics. 1964;**36**: 1050

[10] Scholz T, Scott P, Burke PG. Electron-hydrogen atom scattering at intermediate energies. Journal of Physics B. 1988;**21**:L139

[11] Bhatia AK, Temkin A. Complex-correlation Kohn T-matrix method of calculating total cross sections: Electron-hydrogen elastic scattering. Physical Review A. 2001;**64**:032709

[12] Temkin A. Polarization and triplet electron-hydrogen scattering length. Physical Review Letters. 1961;**6**:354

[13] Bhatia AK. Applications of the hybrid theory to the scattering of electrons from $He^+$ and $Li^{2+}$ and resonances in two-electron systems. Physical Review A. 2008;**77**:052707

[14] Bhatia AK, Temkin A. Calculation of autoionization of He and $H^-$ using the projection-operator formalism. Physical Review A. 1975;**11**:2018

[15] Bhatia AK. Application of P-wave hybrid theory for the scattering of electrons from $He^+$ and resonances in He and $H^-$. Physical Review A. 2007;**86**: 032713

[16] Bhatia AK. Hybrid theory of P-wave electron-$Li^{2+}$ elastic scattering and photoabsorption in two-electron systems. Physical Review A. 2013;**87**: 042705

[17] Oza DH. Phase shifts and resonances for electron scattering by $He^+$ below the N=2 threshold. Physical Review A. 1986; **33**:824

[18] Gien TT. Accurate calculation of phase shifts for electron collisions with positive ions. Journal of Physics B. 2003; **36**:2291

[19] Wildt R. Electron affinity in astrophysics. The Astrophysical Journal. 1939;**89**:295

[20] Ohmura T, Ohmura H. Electron-hydrogen scattering at low energies. Physics Review. 1960;**118**:154

[21] Nahar SN. In: Chavez M, Bertone E, Rosa-Gonzalez D, Rodriguez-Merino

LR, editors. New Quests Stellar Astrophysics. II. The Ultraviolet Properties of Evolved Stellar Populations. New York: Springer; 2009. p. 245

[22] Samson JAR, He ZX, Yin L, Haddad GN. Precision measurements of the absolute photoionization cross sections of He. Journal of Physics B. 1994;**27**:887

[23] Bhatia AK. Hybrid theory and its applications. Atoms. 2018;**6**:7

[24] Bhatia AK. P-wave electron-$Be^{3+}$, $C^{5+}$, and $O^{7+}$ elastic scattering and photoabsorption in two-electron systems. Journal of Atomic, Molecular, Condensate and Nano Physics. 2014;**1**: 2349

[25] Sinha C, Bhatia AK. Laser-assisted free-free transitions in electron-atom collisions. Physical Review A. 2011;**83**: 063417

[26] Bhatia AK, Sinha C. Sinha. Free-Free transitions of the e-H system inside a dense plasma irradiated by a laser field at very low incident-electron energies. Physical Review A. 2012;**86**:053421

[27] Rodhman T, Sudarshan ECG. Doubt and Certainty, Helix Books. Mass: Reading; 1998. p. 64

[28] Anderson CD. The positive electron. Physics Review. 1933;**43**:491

[29] Bhatia AK, Temkin A, Drachman RJ, Eiserike H. Generalized hylleraas calculation of positron-hydrogen scattering. Physical Review A. 1971;**3**:1328

[30] Bhatia AK. Bhatia, positronium-hydrogen scattering, annihilation, and positronium formation. Atoms. 2016; **4**:27

[31] Bhatia AK. P-wave positronium-hydrogen scattering, annihilation, and positronium formation. Atoms. 2017;**5**:17

[32] Bhatia AK, Temkin A, Eiserike H. Rigorous precision p-wave positron-hydrogen scattering calculations. Physical Review A. 1974;**9**:219

[33] Armstrong RI. Electron-hydrogen scattering calculations. Physics Review. 1968;**171**:9

[34] Ferrell RA. Theory of positron annihilations in solids. Reviews of Modern Physics. 1956;**28**:308

[35] Mohorovicic S. Possibility of new elements and their meaning in astrophysics. Astronomische Nachrichten. 1934;**253**:93

[36] Khan A, Ghosh AS. Positronium formation in positron-hydrogen scattering. Physical Review A. 1983;**27**: 1904

[37] Humberston JW. Positronium formation in s-wave positron-hydrogen scattering. Canadian Journal of Physics. 1982;**60**:591

[38] Bhatia AK, Drachman RJ. Photodetachment of the positronium negative ion. Physical Review A. 1985; **32**:1745

[39] Bhatia AK, Drachman RJ. New Calculations of the properties of the positronium ion. Physical Review A. 1983;**28**:2523

[40] Lailement R, Quemerais E, Bertaux J-L, Sandel BR, Izamodenov V. Voyager measurements of hydrogen lyman-α diffuse emission frm milky way. Science. 2011;**334**:1665

[41] Bhatia AK. Photodetachment of the positronium negative ion with excitation in the positronium atom. Atoms. 2018;**7**:2

[42] Mitroy J, Bromley MWJ, Ryzhikh GG. Topical review: Positron and positronium binding to atoms. Journal of Physics B. 2002;**35**:R81

[43] Doolen GD, Nuttal J, Wherry CJ. Evidence of a resonance in $e^+$-H S-wave scattering. Physical Review Letters. 1978;**40**:313

[44] Bhatia AK, Ho YK. Complex-coordinate calculation of $^{1,3}$P resonances in $Ps^-$ using hylleraas functions. Physical Review A. 1990;**42**:1119

[45] Michishio K, Kanai T, Azuma T, Wade K, Mochizuki I, Hyodo T, et al. Photodetachment of positronium negative ions. Nature Communications. 2016;**7**:11060

[46] Humberston JW, Charlton M, Jacobson FM, Deutch BI. On antihydrogen formation in collisions of antiprotons with positronium. Journal of Physics B. 1987;**20**:347

[47] Kauppila WE, Stein TS, Smart JH, Debabneh MS, Ho YK, Dawning JP, et al. Meaurements of total scattering cross sections for intermediate-energy positrons and electrons colliding with helium, neon, and argon. Physical Review A. 1981;**24**:308

[48] Zhou S, Kappila WE, Kwan CK, Stein TS. Measurements of total cross sections for positrons and electron colliding with atomic hydrogen. Physical Review Letters. 1994;**72**:1443

[49] Walters HRJ. Positron scattering by atomic hydrogen at intermediate energies. Journal of Physics B. 1988;**21**: 1893

[50] Gien TT. Total cross sections for positron-hydrogen scattering. Journal of Physics B. 1995;**28**:L321

[51] Wannier GH. The threshold law of single ionization of atoms or ions by electrons. Physical Review. 1953;**90**:817

[52] Klar H. Threshold ionization of atoms by positrons. Journal of Physics B. 1981;**14**:4165

[53] Wigner EP. On the behavior of cross sections near thresholds. Physics Review. 1948;**73**:1002

[54] Sadeghpour HR, Bohn JL, Cavagnero MJ, Esry BD, Fabrikant II, Macek JH, et al. Collisions near threshold in atomic and molecular physics. Journal of Physics B. 2000;**33**: R93